T. Schripp, B. Anderson[1], E. Crosbie[1], R.H. Moore[1], F. Herrmann, P. Osswald, C. Wahl, M. Kapernaum, M. Köhler, P. Le Clercq, B. Rauch, P. Eichler[2], T. Mikoviny[2], A. Wisthaler[2,3], Impact of Alternative Jet Fuels on Engine Exhaust Composition During the 2015 ECLIF Ground-Based Measurements Campaign, Environmental Science & Technology 52 (2018), 4969-4978.

1 NASA Langley Research Center, Hampton, VA, USA
2 Institut für Ionenphysik und Angewandte Physik, Universität Innsbruck, Innsbruck, Austria
3 Department of Chemistry, University of Oslo, Blindern, Oslo, Norway

Impact of Alternative Jet Fuels on Engine Exhaust Composition During the 2015 ECLIF Ground-Based Measurements Campaign

Tobias Schripp[1*)], Bruce Anderson[2)], Ewan C. Crosbie[2)], Richard H. Moore[2)], Friederike Herrmann[1)], Patrick Oßwald[1)], Claus Wahl[1)], Manfred Kapernaum[1)], Markus Köhler[1)], Patrick Le Clercq[1)], Bastian Rauch[1)], Philipp Eichler[3)**], Tomas Mikoviny[4)] and Armin Wisthaler[3,4)]

[1)] German Aerospace Center (DLR), Institute of Combustion Technology, 70569 Stuttgart, Germany

[2)] NASA Langley Research Center, Hampton, VA 23666, USA

[3)] Institut für Ionenphysik und Angewandte Physik, Universität Innsbruck, 6020 Innsbruck, Austria

[4)] Department of Chemistry, University of Oslo, Blindern, 0371 Oslo, Norway

* Corresponding author: tobias.schripp@dlr.de

** Current affiliation: German Environment Agency, 06844 Dessau-Roßlau, Germany

Keywords: aircraft emissions, kerosene, particle emission, non-methane organic gases

Graphical Abstract

Abstract

The application of fuels from renewable sources (“alternative fuels”) in aviation is important for the reduction of anthropogenic carbon dioxide emissions, but may also attribute to reduced release of particles from jet engines. The present experiment describes ground-based measurements in the framework of the ECLIF (Emission and Climate Impact of Alternative Fuels) campaign using an Airbus A320 (V2527-A5 engines) burning six fuels of chemically different composition. Two reference Jet A-1 with slightly different chemical parameters were applied and further used in combination with a Fischer-Tropsch synthetic paraffinic kerosene (FT-SPK) to prepare 3 semi synthetic jet fuels (SSJF) of different aromatic content. In addition, one commercially available fully synthetic jet fuel (FSJF) featured the lowest aromatic content of the fuel selection. Neither the release of nitrogen oxide or carbon monoxide was significantly affected by the different fuel composition. The measured particle emission indices showed a reduction up to 50% (number) and 70% (mass) for two alternative jet fuels (FSJF, SSJF2) at low power settings in comparison to the reference fuels. The reduction is less pronounced at higher operating conditions but the release of particle number and particle mass is still significant lower for the alternative fuels than both reference fuels. The observed correlation between emitted particle mass and fuel aromatics is not strict. Here, the H/C ratio is a better indicator for soot emission.

Introduction

The global aviation sector is projected to grow markedly in coming decades, which will place pressure on the international fuel supply as well as efforts to improve environmental sustainability and reduce the industry’s carbon footprint. In 2016, the United States alone produced 590 million barrels (approx. 94 billion liters) of kerosene-type jet fuel[1], which, although down from its peak in the early-2000s, has been steadily trending upward over the past few years. This has led to increased market interest for alternative jet fuels (such as those derived from bio-based feedstocks) to supplement the traditional, petroleum-based Jet

A-1 (ASTM D1655) now in service. Currently, approved alternative fuels (ASTM D7566) are created by blending regular Jet A-1 with blend stocks from non-petroleum-based sources, which is done for two main reasons. First, the production market of synthetic fuels is immature, which leads to poor economic viability under the current regulatory environment. Second, and most importantly, the alternative fuel must be "drop-in" compatible with all aircraft, including older aircraft fuel systems that were designed based on the Jet A-1 fuel standard. While widespread future adoption of alternative fuels is expected to be driven by reducing the emission of greenhouse gases such as CO_2, these fuels also are expected to have important co-beneficial reductions in the amount of non-CO_2-emissions, such as nitrogen oxides and particles. The formation of particles are of high scientific interest since they are linked to the formation of ice crystals in the atmosphere[2] and – at ground level – may contribute to human particle exposure[3, 4]. Therefore, information about the release of particles with regard to number, size and chemical composition are of high relevance.

Engine particle emissions changes from burning alternative fuels relative to traditional, petroleum-based fuels are thought to be driven by variation in the amount of fuel sulfur and aromatic species. For instance, the Fischer-Tropsch (FT) fuels in the AAFEX-I campaign (2009) and the hydro-processed esters and fatty acids (HEFA) fuel of the ACCESS-I campaign (2013) contained no aromatic compounds and nearly no sulfur[5]. They were used in blends with regular JP-8 fuel (which differs from Jet A-1 solely by its additives) and led to a significant decrease in emitted particles with increasing alternative fuel content. Brem et al. showed that increasing the content of aromatics in regular Jet A-1 fuel led to an increased particle emission of a jet gas turbine[6]. Experiments with a T63-A-700 turboshaft engine showed a reduction of particle emission when changing from regular JP-8 to a mainly paraffinic fuel[7, 8]. The authors further showed that the emitted particle number was reduced but the formation mechanism and the growth behavior of the soot was similar. Comparable experiments on a PW308 engine revealed a significant particle reduction at lower power settings if JP-8 was blended with an aromatic free FT fuel.[9]

Therefore, the reduction of soot precursors is a possible explanation of the observed decrease in emission. While there have been a number of past, ground-based studies attempting to quantify the emissions impacts associated with alternative fuels (e.g., AAFEX and ACCESS), these studies only examined a few fuels where the fuel sulfur and aromatic content co-varied together. Consequently, there is a need to better understand and quantify the impact of systematically varying fuel aromatic content on engine particle emissions.

The experiments presented in this paper address this knowledge gap and were performed in the framework of the ECLIF (Emission and Climate Impact of Alternative Fuels) campaign of the German Aerospace Center and the US National Aeronautics and Space Administration. ECLIF consisted of a series of flight and ground measurements in combination with fuel characterization experiments. The present study provides a unique investigation of the fuel impact on full scale aero engine emissions. The systematic variation of the fuels composition, primarily the aromatic content, within the range of present jet fuel specifications (ASTM D1655[10] and D7566[11]) has permitted ground and inflight (not shown in this paper) measurements of the exhaust of an Airbus A320 while burning six fuels of chemically different composition.

Materials and Methods

Fuels

Six different fuels were investigated during ECLIF, which are shown in Table 1, along with the targeted fuel blending ratios. All six fuels were supplied by Sasol as certified jet fuels. Two, petroleum-based Jet A-1 fuels from the NatRef refinery (South Africa) were used. The reference fuel Ref1 consisted of 100% Merox product while Ref2 consisted of 82% Merox (mercaptan oxidation) and 18% DHC (distillate hydrocracking). Ref2 was produced while the refinery was operated to deliver fuel and bitumen ("Bitumen run"). This led to slight variations in the composition, like, e.g. Ref1 had a slightly lower sulfur content (1170 ppm) than Ref2 (1354 ppm). However, the differences in the chemical composition end up being minimal. Ref1 features some paraffins with higher chain-length but the overall H/C ratio is nearly identical to Ref2. Three additional fuels were purchased from Sasol while one fully synthetic jet fuel (FSJF) was donated by Sasol. The FSJF was a mixture of fuels from different processes. Sasol used one synthetic paraffinic kerosene (SPK) type fuel in order to prepare three ("semi-synthetic") blends with the reference Jet A-1 fuels (SSJF1-3) to achieve different aromatic contents. The main goal was having a broad range of aromatic contents – and possible particle formation potential - while still complying with ASTM specifications. The fuel descriptions are summarized in Table 1, and their specifications are detailed in Table 2. The fuels were stored in regular iso-containers on the Manching airfield before fueling.

Table 1: Summary of investigated fuels and blends.

Short	Fuel	Aimed composition
Ref1	Reference kerosene 1	100% Jet A-1 (Merox)
Ref2	Reference kerosene 2	100% Jet A-1 ("Bitumen Run")
SSJF1	Semi-synthetic jet fuel 1	59% Ref1 + 41% SPK
SSJF2	Semi-synthetic jet fuel 2	55% Ref2 + 45% SPK
SSJF3	Semi-synthetic jet fuel 3	86% Ref1 + 14% SPK
FSJF	Fully synthetic jet fuel	100% FSJF

Comprehensive two-dimensional gas chromatography (GCxGC) was used to provide information about the test fuel chemical compositions and to determine hydrogen to carbon ratios (H/C) for each test fuel. This method applies two independent separations to a single sample injection and is considered to be the most accurate means to obtain detailed compositional information for complex petrochemical mixtures. Complex fuels are traditionally analysed in the so-called "normal" GCxGC mode where a non–polar column is used in the first dimension to perform a boiling-point based separation. The effluent from the first column is focussed onto a polar column, which provides separation in the second dimension based on polarity. For this study the so-called "inverse mode" was employed where the first dimension employs a polar column and the second dimension employs a non–polar column. This sequence is considered to normally be less orthogonal but has been demonstrated to extend the separation space when used to characterise FT fuels and the aromatic fractions in petroleum middle–distillates resulting in improved resolution. Time–of–flight mass spectrometry (TOF–MS) was used to identify chemical structures, and a flame ionisation detector (FID) was used for quantification.

Table 2: Properties and composition (analysis by the manufacturer) of the fuels.

	Ref1	Ref2	SSJF1	SSJF2	SSJF3	FSJF
C (ASTM D 5291) [mass%]	84.8	85.5	n.d.	84.0	85.0	85.0
H (ASTM D 5291) [mass%]	14.1	14.1	n.d.	14.7	14.2	14.5
Heat of combustion (ASTM D240) [kJ/g][a)]	42.800	43.200	43.496	43.540	43.301	43.330
Smoke point (ASTM D 1322) [mm][b)]	25.0	26.0	26.0	26.0	25.0	25.0
Total sulfur content* [mass%][c)] (ASTM D2622 IP 336)**	0.117 (0.10)	0.135 (0.10)	0.057 (0.05)	0.070 (0.06)	0.159 (0.08)	<0.01 (<0.01)
Density at 15°C (ASTM D4052) [kg/m³][d)]	812.7	808.9	790.2	783.4	803.2	807.9
Aromatics (ASTM D1319) [vol%][e)]	18.0	17.2	11.4	10.9	15.3	8.9
H/C ratio*	1.922	1.925	2.029	2.045	1.954	1.981
n-Paraffins* [mass%]	22.15	25.38	14.01	11.75	20.17	3.70
iso-Paraffins* [mass%]	23.40	21.67	54.00	60.97	32.30	49.71
monocyclic-Paraffins* [mass%]	23.24	22.63	14.47	11.82	20.55	13.15
bicyclic-Paraffins* [mass%]	9.25	8.75	5.16	4.38	7.87	16.41
tri-, polycyclic-Paraffins* [mass%]	1.50	1.34	0.76	0.38	1.27	7.71
n-, iso-Alkylbenzenes* [mass%]	13.46	13.26	7.77	7.52	11.72	3.72
cyclo-Alkylbenzenes* [mass%]	4.47	3.71	2.40	1.72	3.97	5.40
bicyclic-Aromatics* [mass%]	2.44	3.22	1.40	1.45	2.09	0.20

Specifications in ASTM D1655[10]: a) >42.8 kJ/g; b) >25.0 or >18.0 and naphthalenes <3.0 vol%; c) <0.30 m%; d) 775 – 840 kg/m³; e) <25 vol% (D1319 method). * from GCxGC fuel analysis (Sasol); ** data from manufacturer data sheet.

All fuels in this study are mainly composed of paraffinic compounds (80 mass% - 90 mass%) but exhibit significant variability in aromatic content, which is driven mainly by the aliphatic residues of benzene. FSJF is an exception, where the amount of bicyclic aromatics is significantly lower than the remaining fuels. This decrease in bicyclic aromatics does not

appear to affect the measured FSJF smoke point, which is often considered a rough indicator for sooting behavior.

Experimental setup

The ground measurements were performed on 8 days between 21 September 2015 and the 08 October 2015 on the airfield of the Technical and Airworthiness Center for Aircraft of the German Armed Forces (Bundeswehr) in Manching, Southern Germany. The experiments were conducted at ambient air temperatures between 16°C and 22°C and wind speed conditions between 1.2 km/h and 8.7 km/h.

The experiments were performed with the Airbus A320-232 D-ATRA (Advanced Technology Research Aircraft) of the German Aerospace Center. The aircraft is equipped with two IAE V2527-A5 engines. The ATRA continuously records approx. 100 system parameters (e.g. fan speed N1, fuel flow, etc.) allowing a correlation between setting and measured exhaust emissions. The aircraft was filled with the target fuel(s) and a flight measurement was performed (data not shown). The ground measurements were performed directly after landing. The fuels Ref1, Ref2, SSJF1 and SSJF2 were tested in both engines on the same day. On the remaining days, the fuels in the two engines were different (see Table S1 for details). The inner and outer wing tank for each engine was filled with approx. 3 metric tons fuel per test. The center tank was not used for the experiment and all cross-feed valves were closed (no fuel switch). After filling the tank, fuel samples are collected from each tank and then analyzed to account for any fuel contamination and slight alteration of its composition from any small amount of residual fuel in the tanks. Significant variation in the fuel properties, especially the aromatic content have not been observed except a single sample of engine 1. However, no abnormalities have been observed in the respective exhaust measurements and we thus consider no cross contamination of the burned fuels. The aircraft was operated at five different power settings (Table 3). It must be noted that the pilots operated the aircraft at the same fuel flow for each power setting and, thus, fan speed and thrust may differ due to different environmental conditions. The parameters in Table 3 represent ground measurements and are not necessarily transferable to inflight conditions. Both engines were always running at the same speed to avoid movement or distortion of the aircraft. Each test point was measured for approx. 3 min (2 min for MCT). The analysis in this paper solely focus on the results from engine 2 (right engine) and, thus, each fuel is presented without a repeat measurement on a different day.

Table 3: Correlation between N1 fan speed, thrust and fuel flow at the different operating points as recorded by the ATRA flight recorder.

Operating point	**Fuel flow [kg/s]**	**N1 speed**		**Thrust**[a)]	
		[RPM]	**[%]**	**[kN]**	**[%]**[b)]
Idle	0.107	1301	20	8	7
Intermediate Point 1	0.205	2235	35	18	17
Intermediate Point 2	0.431	3373	53	44	39
Intermediate Point 3	0.703	4211	66	74	66

Maximum Continuous Thrust (MCT)	0.900	4611	72	96	86

a) Estimated from the ICAO data sheet for the used V2527-A5 engine; b) max. 111.2 kN

Sampling and particle analytics

Two stainless-steel sampling probes were installed 30 m behind the two engines at a height of approximately 1 m (Figure S1). The sampling line was unheated and featured a tube outer diameter of 1.9 cm (3/4''). The sampling line from each probe was connected to a valve box to switch between the two engine exhausts. The tube length between sample inlet and valve box was identical for both lines to ensure similar residence times. Behind the valve box, the line was split between the NASA and DLR instruments. The total sample transfer time for both groups was similar (DLR: 22 seconds, NASA: 18 seconds).

The particle number concentration was determined with a TSI 3022A CPC (particle diameter, D_p > 7 nm), a TSI 3775 CPC (D_p > 4 nm) and a TSI 3776 CPC (D_p > 2.5 nm). Time-resolved measurements were performed with a TSI Scanning Mobility Particle Sizer (SMPS) consisting of a 3082 electrostatic classifier, a 3081 long-DMA, a 3088 x-ray neutralizer and a 3776 CPC. The SMPS measured the size distribution in the range 9-256 nm over a 45-second scan time. In addition, a TSI Engine Exhaust Particle Sizer (EEPS) measured the size distribution in the range 5.6 – 560 nm at 10 Hz. The aerosol for the SMPS and the CPC 3775 could be switched to be measured directly or pass through a self-developed thermodenuder operating at 350°C. The aerosol for the EEPS and the 3776 CPC were diluted with a DI-1000 Dekati Diluter (1:30) using compressed nitrogen while the aerosol for the CPC 3022A was further diluted to get a dilution of 1:60 (see Figure S1). The dilution aimed to prevent the CPCs to switch from single-counting mode into photometric mode[12]. The soot particles were also determined with an Aerodyne Cavity-Attenuated Phase Shift (CAPS) extinction monitor operating at 660 nm (mass absorption coefficient 7 m²/g).

The particle mass concentration was calculated from the EEPS and SMPS data by assuming spherical particles with a density of 1.07 g/cm³ (see "Particle emission" section for details). Due to noise artifacts in the EEPS (see "Particle emission" section), a cutoff diameter of 154 nm is used for the particle mass analysis. The calculation of the emission index for particulate emissions (equation 1) and combustion gases (equation 2) follow the approach in AIR6037 Appendix D[13] using the obtained particle number concentration (PNC), particle mass concentration (PMC) or gas concentration [gas], the measured concentration of carbon dioxide in air ([CO2]), the background carbon dioxide concentration ($[CO2]_{BG}$), the concentration of carbon monoxide ([CO]), the current atmospheric pressure at the instrument inlet (p), the molar ratio of hydrogen to carbon in the fuel (α) and the molar masses of carbon (M_C) and hydrogen (M_H). The combustion gases (e.g. carbon dioxide, nitrogen oxides, etc.) were monitored with a MKS MultiGas 2030 FTIR Continuous Gas Analyzer.

$$EI\left[\frac{\#}{kg}\ \text{or}\ \frac{mg}{kg}\right] = \frac{PNC\ \text{or}\ PMC[\frac{\#}{m^3}\ \text{or}\ \frac{mg}{m^3}]\cdot R[\frac{m^3 atm}{K\,mol}]\cdot T[K]\cdot 10^3}{[CO2]-[CO2]_{BG}+[CO]} \cdot \frac{1}{M_C[\frac{g}{mol}]+\alpha M_H[\frac{g}{mol}]} \cdot \frac{1}{p[atm]} \quad (1)$$

$$EI\left[\frac{g}{kg}\right] = \frac{[gas]}{[CO2]-[CO2]_{BG}+[CO]} \cdot \frac{R[\frac{m^3 atm}{K\,mol}]\cdot T[K]\cdot 10^3}{p[atm](M_C[\frac{g}{mol}]+\alpha M_H[\frac{g}{mol}])} \cdot \frac{M_{gas}[\frac{g}{mol}]}{V_m[\frac{m^3}{mol}]} \quad (2)$$

The majority of the particle data shown in this article are based on non-treated aerosol measurements. Therefore, the term “particle” is meant as “total particle”. In case of a thermally treated aerosol (thermodenuder), the term “non-volatile particle” is used.

Volatile organics

Non-methane organic gases (NMOGs) were sampled from the same sampling point as particles but through separate inlet lines (length: 30 m, outer diameter: 6.35 mm, material: Teflon PFA, sampling flow: ~5 slpm, temperature: 80 °C). NMOGs were measured using a Proton-Transfer-Reaction Time-of-Flight Mass Spectrometer (PTR-TOF 8000, Ionicon Analytik GmbH). The drift tube was operated at 2.20 mbar absolute pressure, a temperature of 110 °C, and a reduced electric field strength of 120 Td ($1.2 \cdot 10^{-15}$ V·cm^2). Data were recorded and analyzed at 1 s time resolution. The data analysis was limited to 12 target compounds (m/z signal and measurement accuracy given in parentheses): formaldehyde (m/z 31.018; ±50%), acetaldehyde (m/z 45.033; ±10%), acrolein (m/z 57.033; ±20%), acetone and propanal (m/z 59.049; ±10%), crotonaldehyde (m/z 71.049; ±20%), benzene (m/z 79.054; ±5%), toluene (m/z 93.070; ±5%), benzaldehyde (m/z 107.049; ±20%), C8-alkylbenzenes (m/z 107.085; ±5%), C9-alkylbenzenes (m/z 121.101; ±5%), tolualdehyde (m/z 121.065; ±20%), and naphthalene (m/z 129.070; ±20%). The PTR-TOF 8000 instrument was calibrated on site using a dynamically diluted multicomponent NMOG standard (Apel Riemer Environmental Inc.) which included approx. 1 ppm of acetaldehyde, acetone, benzene, toluene, m-xylene, and 1,3,4-trimethylbenzene, respectively. Instrumental response factors for formaldehyde, acrolein and crotonaldehyde had been obtained in previous work using the same instrument. Response factors for benzaldehyde, tolualdehyde and naphtalene were calculated using ion-molecule collision theory. Carbon dioxide (CO_2) was measured from the same inlet line using a non-dispersive infrared gas analyzer (model LI-820, LI-COR Biosciences).

Results and Discussion

Emission of combustion gases and volatile organics

The fuels containing synthetic kerosene could be used in the aircraft without significant changes in operation conditions, such as, fuel flow or exhaust gas temperature. As a result, the combustion gas emissions are similar for all tested fuels (Figure 1). The nitrogen oxide emission rises with increasing fuel flow (Figure 1B) which corresponds to higher temperatures in the combustion chamber and in the exhaust gas. Small deviations of NO_x emission at low power settings appear to be related to the ambient conditions rather than to the fuel composition. This allows for the conclusion that the changes in fuel composition do not change the flame structure in the combustor as intended by the strict jet fuel specifications. In contrast to the nitrogen oxides, the release of carbon monoxide is mainly relevant (EI > 1 g/kg) for fuel flows < 0.4 kg/s (Figure 1A). This insufficient burning of the fuel at low operation conditions matches the observation of higher organics in the exhaust gas under these conditions (see below). The determined combustion gas emission indices match the ICAO Aircraft Engine Emissions Database[14]. For the nitrogen oxides and the respective engines it reports 26.5 g/kg (T/O, fuel flow 1.05 kg/s) and 4.7 g/kg (idle, fuel flow 0.13 kg/s). The respective values for carbon monoxide are 0.53 g/kg (T/O) and 12.43 g/kg (idle).

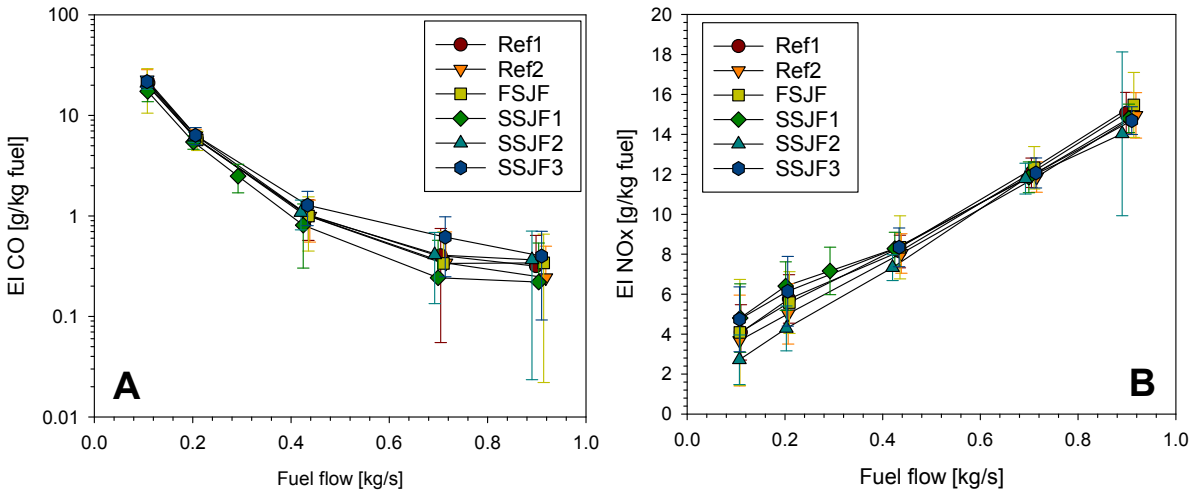

Figure 1: Development of the carbon monoxide emission index (A) and the nitrogen oxides emission index (B) in dependence of fuel flow and fuel type. For each setting the mean over all repetitions in the right engine (engine 2) is shown.

Non-methane organic gases (NMOG) concentrations in the exhaust of the V2527-A5 engine were found to be above ambient background levels only at idling condition, i.e. at a fuel flow of 0.11 kg/s. NMOG enhancements in the exhaust plume were small (ppts to single-digit ppbs) and no statistically significant differences were observed when the engine was operated with different fuels. It should, however, be pointed out that even within the one-minute measurement interval for a specific fuel condition, the variability in the NMOG data ranged from ±10% to ±55%. Small differences in NMOG emissions between different fuel conditions would thus not have been detectable. The high variability was caused by turbulence-induced concentration variations in the sample and a poor measurement precision at ppt level concentrations. We herein report emission indices as measured approx. 10 minutes after engine start when the high pressure compressor exit temperature in the engine (T3) and the exhaust gas temperature were at steady state (~180 °C and ~460 °C, respectively) at idle setting. Average emission indices (in mg/kg fuel) were as follows: formaldehyde 28.9, acetaldehyde 12.9, acrolein 9.1, acetone plus propanal 5.2, crotonaldehyde (plus isomers) 4.6, benzene 7.0, toluene 2.1, benzaldehyde 2.6, C8-alkylbenzenes 3.0, tolualdehyde (plus isomers) 1.8, C9-alkylbenzenes 1.0, naphthalene 0.4. We note that emissions of aldehydes and aromatics are one to two orders of magnitude lower than reported for other jet engines[15]. According to the ICAO Aircraft Engine Emissions Database[14], the V2527-A5 engine emits 105 mg/kg fuel of total hydrocarbons at idle conditions. This is much less than other engine types which typically emit hydrocarbons at g/kg fuel levels. The emission indices given above sum up to 79 mg/kg fuel, which is in reasonable agreement with number reported in the ICAO database. Herndon et al.[15] report formaldehyde emission indices in the range between 40 and 80 mg/kg for a V2527-A5 engine fueled at 0.11 kg/s. The lower values are within the uncertainty of our formaldehyde measurements (±40%). It must be noted that the quantification of formaldehyde with PTR is associated with high uncertainties[16]. The emission measurements also included short idling periods after the engine had been operated for >30 minutes at different thrust levels. Engine and exhaust gas temperatures were, however, not a steady state during these idling phases and the experiment and measurement protocol was not exactly identical for the various fuel conditions. Idling emission indices for the hot engine were typically a factor of 1.5 to 3 lower than those reported above.

Particle emission

Particle number and particle mass emission profiles for the different fuels could be determined with a variability of ~16% which allows discrimination of the particle release of the fuels tested. The comparability between the different particle monitors is complicated by the different size range covered and the different measuring principles (e.g. CAPS). The EEPS was selected as a basis of analysis since the recorded particle size distributions cannot be biased by sudden changes in the aerosol, the size range covers the main modes of emission and the time resolution was sufficient. A correlation analysis between the applied devices is shown in the SI. With reference to the chemical nature of the particles, the volatile fraction of the particles is negligible (Figure S6). This might be caused by the distance between emission source, sampling port and analytics since at a distance of > 20 m the aerosol already aged and the volatile species might have been evaporated[17]. As a result, the comparison between black-carbon measurements (CAPS) and total particle mass (EEPS) indicate that the vast majority of the detected particles represent soot (Fig S5). A consistent reduction in the black carbon mass and non-volatile particle number concentration is observed with increasing fuel H/C ratio (Figure 2A and 2B). There is a clear stratification in the magnitude of soot mass emission indices between high (>0.4 kg/s) and low (<0.4 kg/s) fuel flow, however the trend with H/C is consistent at all power settings. For soot particle number emission indices, the trend is consistent. However, the stratification with power setting is less apparent. Comparisons between the CAPS black carbon mass and integrated non-volatile particle volume indicate good closure with a bulk effective density of 1.07 g/cm^3 (Figure 2C). This agrees well with the observations by Durdina et al.[18] who report a bulk effective density ranging from ~1.10 g/cm³ (ground idle) to ~0.90 g/cm³ (take-off) with a mean effective density of 0.93 ± 0.02 g/cm³ (SMPS) while measuring the exhaust of a CFM56-7B26/3 engine. Since the present study did not cover the highest power settings, the mean bulk density is near to the lower range observed in the mentioned study.

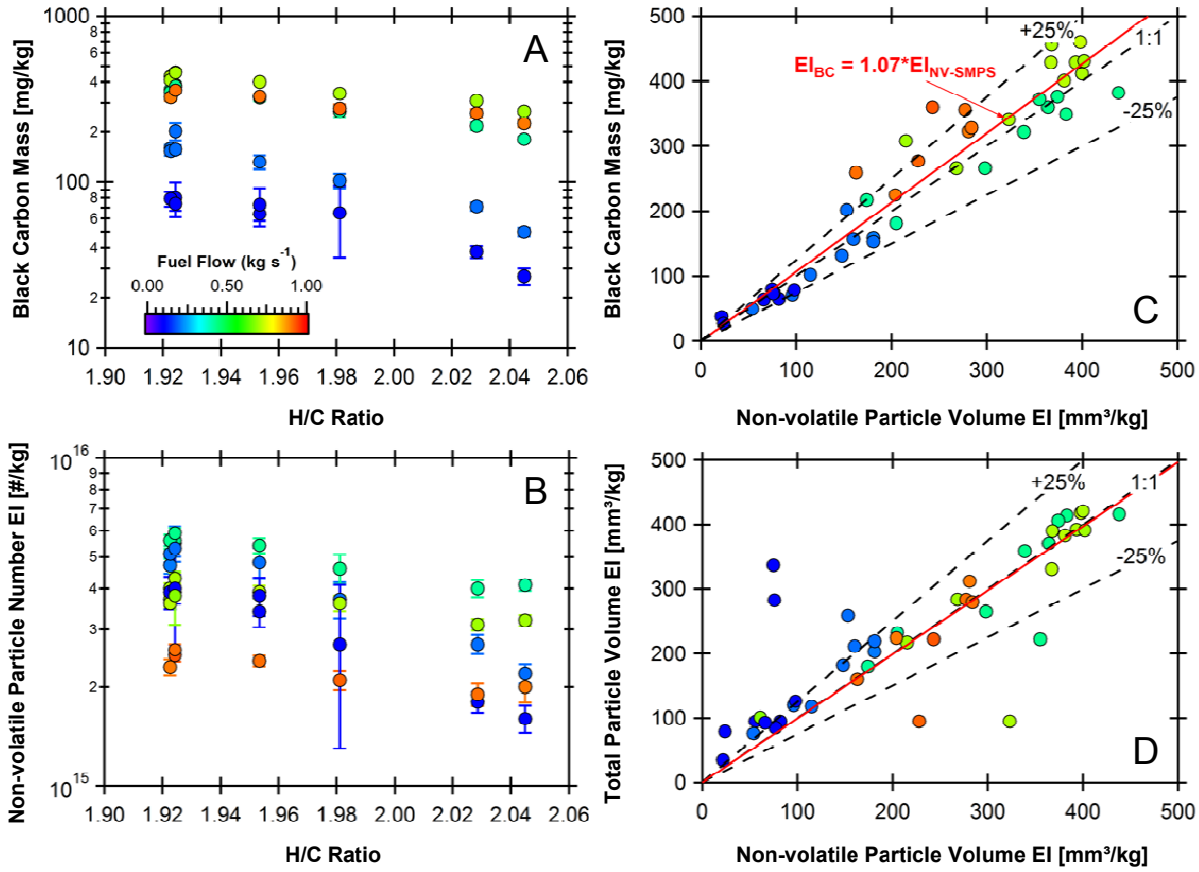

Figure 2: Black carbon mass EI (A) from the CAPS and mean non-volatile particle number EI from the thermal-denuded CPC (B) plotted versus the fuel H/C ratio. One-to-one plot of BC mass EI vs. non-volatile particle volume EI from the SMPS (C) and one-to-one plot of total vs. non-volatile particle volume EIs (all fuels) both from the SMPS (D). All points are for Engine #2 and are colored by the fuel flow rate as shown in (A). Red, solid lines on the one-to-one plots are linear fits to the data.

With regard to the number of emitted particles (Figure 3A), the highest influence of the synthetic fuels is observed for low operating conditions (fuel flow <0.4 kg/s). Here, the FSJF and SSJF1 showed a reduction of 50 – 60% in comparison to the reference Jet A-1 kerosene Ref1. This reduction is still ~30% at the highest operating condition. The mass size distribution (Fig 4 and SI) shows one distinct mode and a shift in the mass median diameter from 50 nm to 70 nm for most fuels. In case of SSJF2, however, the shift is far less distinctive (from 60 nm to 64 nm). Both mass size distributions (Figure 4B and 4D) show an increase for particles >200 nm. This has been also reported by Durdina et al.[18] who observed a mode between 200 and 500 nm with elevated mass concentration and low particle number concentration. The authors attributed this mode to a measuring artifact. Therefore, a cutoff diameter of 154 nm has been selected for this study (e.g. Figure 3B). It is important to note that the observed particle number size distribution is bimodal for all fuels (see Figure 4A and 4C) which hinders a comparable interpretation via the count median diameter. One particle number mode features a peak at ~10 nm (nucleation mode) while the second peaks at 40 – 50 nm (accumulation mode). This particle size distribution has been reported by several other publications[19-22]. The sulfur content in the fuel has a direct impact on the nucleation particle mode at sufficient distance from the engine exhaust (>15 m)[23]. This is in good agreement to the particle number size distributions in the present measurements (Figure 4 and Figure S7-S14) but the impact of the particle mode at 10 nm on the total emitted particle

mass is – of course – negligible (Figure 4B and 4D). Therefore, a correlation between emitted particle mass and the sulfur content cannot be observed. It should be noted that Lobo et al.[20] indicate that the bimodal size distribution is less pronounced for the A320 with V2500-A5 engines (~70% of particles in nucleation mode) than in case of other engines studied. From experimental studies, Vander Wal et al.[24] concluded that the nanostructure of the soot transforms from an amorphous structure at low power settings to a "graphitic" structure at high power settings. The first mode is highest for Ref1 (highest aromatic content) and lowest for the FSJF (lowest aromatic content, Figure 4C). The shift in the MMD leads to similar reduction rates of 50 – 70% (lowest setting) and approx. 20% (highest setting) for SSJF2 if particle mass is considered. The correlation between particle mass emission and aromatic content is not strict (Figure 5A) because the FSJF shows a higher emission than anticipated from the aromatic content. Furthermore, the deviation in emission of the SSJF2 to the SSJF1 is larger than expected. However, the particle mass emission correlates well with the H/C ratio of the fuels (Figure 5B).

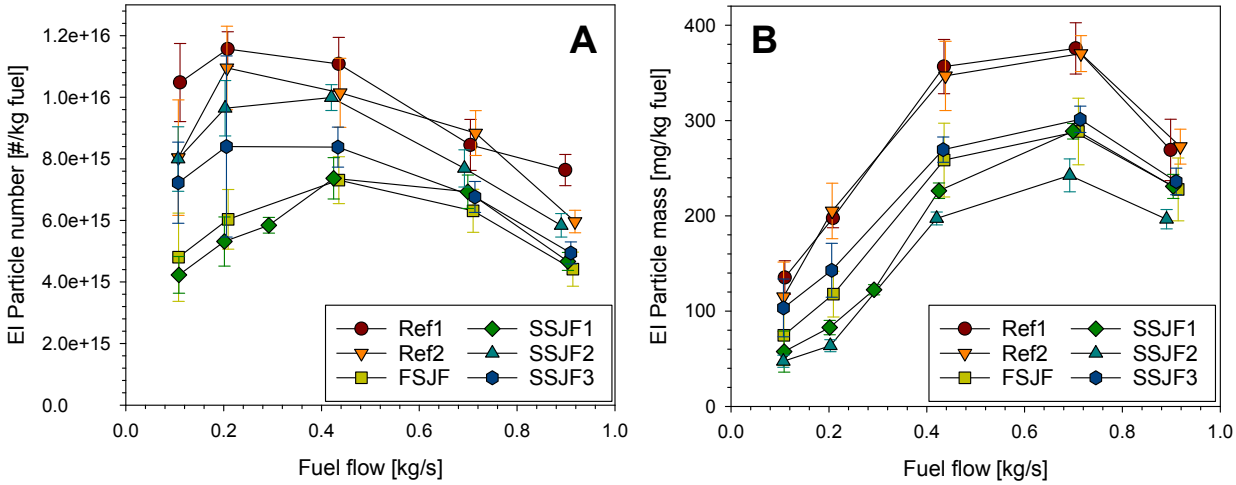

Figure 3: Development of the particle number (EEPS) emission index (A) and the particle mass (EEPS) emission index (B) in dependence of fuel flow and fuel type. For each fuel flow only results from the right engine (engine 2) are shown.

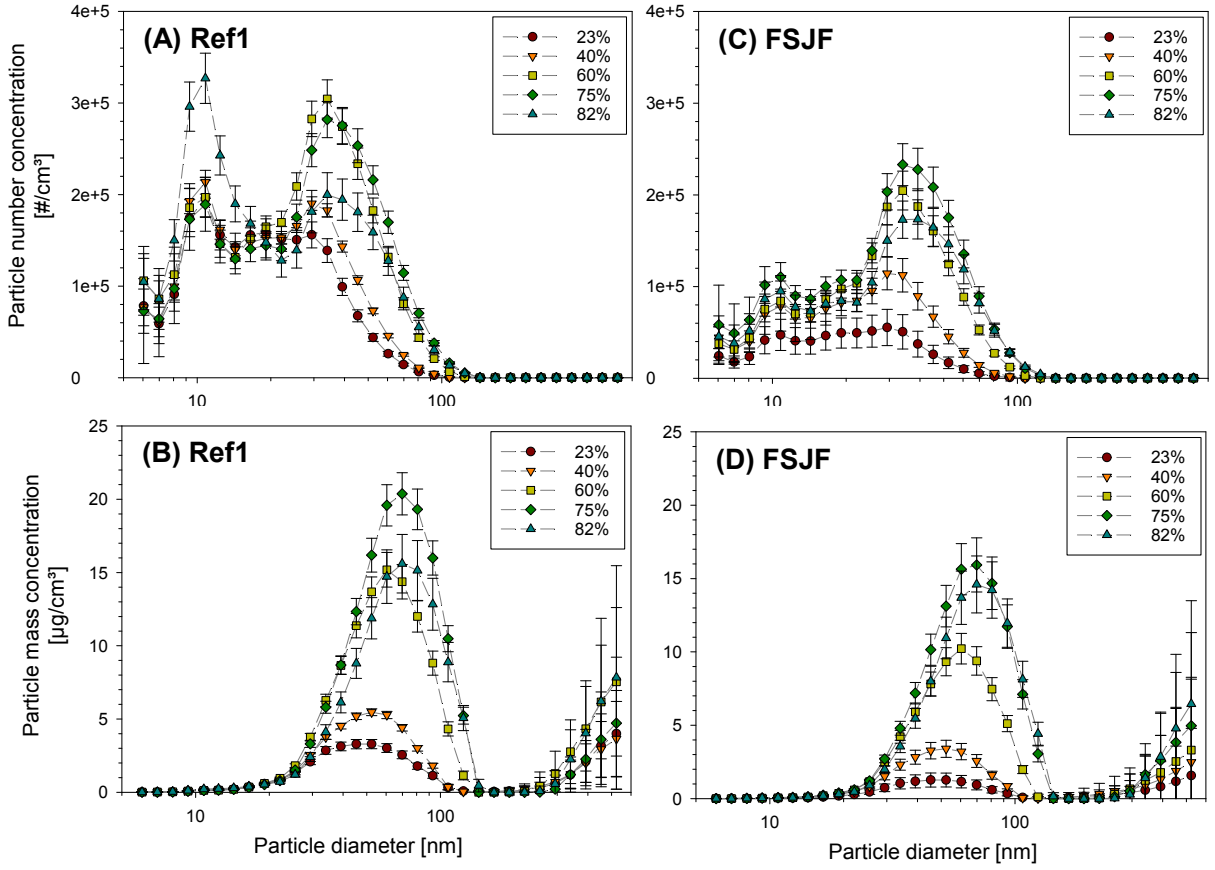

Figure 4: Particle size distributions (EEPS) for the fuels Ref1 (highest aromatics) and FSJF (lowest aromatics) at different power settings. The particle number distributions are given in (A) and (C) while the particle mass distributions are given in (B) and (D).

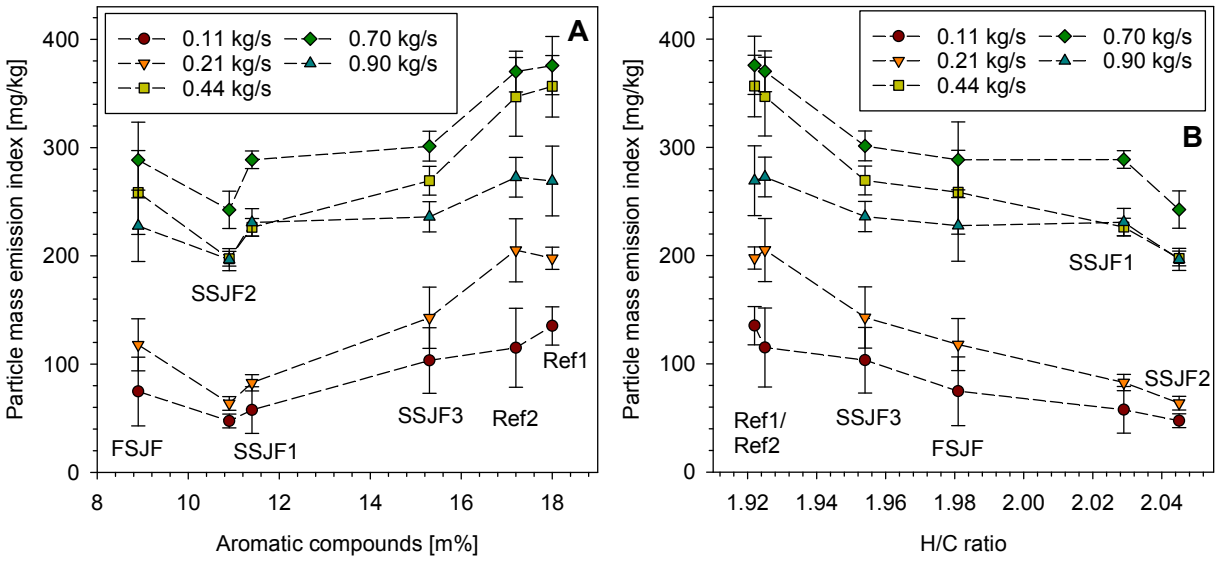

Figure 5: Influence of the content of fuel aromatics (A) and the H/C ratio (B) on the particle mass emission index (mean) of engine 2 at different fuel flows.

Comparison to previous findings, limitations of the study and combustion chemistry

In order to compare the present particle findings with other studies, the black carbon emission at the engine exhaust was calculated on the basis of the air-to-fuel ratio (AFR, eq. 14 in Ref.[25]), the EEPS particle mass emission index and a bypass ratio (BPR) of 4.82 for the V2527-A5 engine (ICAO database[14]). The results were compared with the estimated black carbon concentration based on the smoke number (ICAO database) of the engine using the respective correlation function (equation D-2 in ICAO 9889[26]). For the low operating conditions and the highest operating condition a good correlation to the expected value is given (Figure S17). For the intermediate operating conditions a higher concentration was observed than anticipated from the smoke number. This might be caused by aging effects of the engine (Figure S18). However, the results indicate that emission indices obtained from the EEPS data are in the expected range for the engine under test. During the monitoring of particle emissions of regular LTO operation on the Oakland airport Lobo et al.[20] observed $1 \cdot 10^{16}$ #/kg – $4 \cdot 10^{16}$ #/kg (idle), 500 mg/kg – 600 mg/kg (idle), $6 \cdot 10^{16}$ #/kg – $9 \cdot 10^{16}$ #/kg (T/O) and 300 mg/kg – 350 mg/kg (T/O) for the Airbus A320 equipped with V2500-A5 engines. In the present study, the values for PN and PM are lower and there is significant deviation for idle conditions – which might be caused by the different sulfur content of the respective fuels. Furthermore, Mazaheri et al.[19] report emission indices for the A320 during measurements at the Brisbane airport of 3.6 g/kg (NO_x), $6.6 \cdot 10^{15}$ #/kg (PN) and 140 mg/kg (PM) for taxi (fuel flow 0.3 kg/s) as well as 17.2 g/kg (NO_x), $2.1 \cdot 10^{16}$ #/kg (PN) and 230 mg/kg (PM) for take-off (fuel flow 1.05 kg/s). These values are in good agreement to the results of this study. Nevertheless, the emission indices of the present static ground measurements do not necessarily match to real start operations where non-transient operation conditions are given.

Overall, a significant reduction of particulate emissions - primarily identified as non-volatile black carbon - has been observed for the (semi-)synthetic fuels. A reduction of up to ~70% in particle mass has been observed. This is consistent with previous studies where reductions of particulate emissions have been related with the fuels lower aromatic content or higher H-content respectively[5, 6, 27]. Typically, the H-content or H/C ratio are used synonymously with the total aromatic content since aromatic molecules constitutionally exhibit a low hydrogen content (H/C ~ 1:1) compared to aliphatic hydrocarbons (H/C ~ 2:1). Within the available sources of present jet fuels - including the typically highly aliphatic alternative fuel blends (HEFA, ATJ) - an independent variation of H/C ratio and aromatic content is barley possible. For instance, Christie et al. illustrated the missing correlation between aromatic content and H/C ratio for 65 commercial jet fuels in the range between 1.84 - 2.00 for H/C and 15-23% for aromatics[28]. The FSJF in the present study, however, combines low total aromatics content with relatively high carbon content (or high H/C ratio respectively) and thus allows a direct comparison with the semi synthetic fuels where the aromatic content is reduced by a dilution with hydrogen-rich aliphatic compounds. Indeed the soot emission reduction - in terms of particle mass - is less pronounced for the FSJF than for SSJF1 and SSJF2 which exhibit nearly the same aromatic content (Figure 5A). Thus, the H/C ratio appears to be a better measure for the sooting tendency than the aromatic content - at least for the present study (Figure 5B).

Presupposed the flame conditions and structure of the engine's combustor are actually not affected significantly by the fuel composition, the soot emission of the engine is dominated by chemical reaction/oxidation characteristic of the respective fuel and its chemical composition. When comparing the composition of FSJF and SSJF1 the most outstanding difference is the high amount of cyclic aliphatic compounds in the FSJF. Indeed, fundamental flame investigations of pure cycloalkanes, like, cyclohexane[29], p-menthane[30] or decalin[31] proof an

increased amount of soot precursor species within their intermediate species pool. Six-membered cycloalkanes are known to exhibit a reaction pathway by consecutive dehydrogenation which is forming phenylic structures. This is an additional pathway to form soot precursor species as benzene and PAHs while larger normal- and iso-alkanes form soot precursor specs solely after decomposition to C2-C4 building blocks[32]. Roughly, the sooting tendency decreases from aromatics via cycloalkanes and iso-alkanes to n-alkanes. This order of sooting tendency can in principle also be seen from smoke point measurements of pure substances. However, the rating of fuels via smoke point may fail – as seen in this study – due to the complex interaction of various fuel properties influencing soot formation. Further lab scale experiments, such as optically accessible, semi technical swirl flames[33] and direct investigation of the chemical reactions[34] of these complex fuels are needed to determine the underlying chemo-physical processes responsible for the observed particle reduction.

The investigation of the engine emissions using six different systematically designed jet-fuel compositions illustrates the abilities of soot reduction at the aviation sector. However, the results are associated with certain limitations. The duration of the power settings in this study was insufficient to discriminate total particle emission and non-volatile particle emission via SMPS at the desired precision. Due to the unexpected high variation in the performance of both engines, future measurements have to be performed with the same engine in order to determine the impact of different fuels. As indicated by the non-strict trend between particle mass emission and fuel aromatic content, future studies have to focus more on the precise chemical composition of these aromatics in jet fuels. Until then, the H/C ratio seems to be the best indicator for soot emissions since it is a better predictor for the combustion chemistry[35]. The mentioned limitations have been considered in the design of the follow-up campaign (NASA/DLR Multidisciplinary Airborne Experiment, ND-MAX/ECLIF) which has been performed in 2018. These high-effort campaigns illustrate the necessity for future scientific progress in fuel design and analytical procedures in order to minimize impact of aviation on climate and human health.

Acknowledgements

This work has been funded by the DLR aeronautics program in the framework of the project “Emission and Climate Impact of Alternative Fuels (ECLIF)”. The authors sincerely thank Sasol for donating the fully synthetic jet fuel and for providing the GCxGC content analysis of all fuels. The authors are grateful to Hans-Jürgen Berns and Stefan Seydel (pilots), Adrian Müller and Waldemar Krebs (flight test engineers), Stefan Schröder (logistics), Tina Jurkat-Witschas (probe design and measuring support) and André Krajewski (flight test planning and fuel logistics) for their commitment to a successful measuring campaign. The authors acknowledge the Bundeswehr, especially Peter Pörsch and David Cyrol, for hosting the experiment at Manching airport and their on-site support. AW acknowledges support by the Austrian Federal Ministry for Transport, Innovation and Technology (bmvit) through the Austrian Aeronautics Program TAKE OFF of the Austrian Research Promotion Agency (FFG, Project no. 855214).

Supporting Information

The Supporting Information contains additional information on the test matrix, environmental conditions, instrument correlation, particle size distributions and difference between the right and left engine. The emission indices are also given in tabular form.

References

(1) U.S. Energy Information Administration
https://www.eia.gov/dnav/pet/pet_cons_psup_dc_nus_mbbl_a.htm (11/2017).
(2) Kärcher, B., The importance of contrail ice formation for mitigating the climate impact of aviation. *J. Geophys. Res.-Atmos.* **2016,** *121*, (7), 3497-3505.
(3) Buonanno, G.; Bernabei, M.; Avino, P.; Stabile, L., Occupational exposure to airborne particles and other pollutants in an aviation base. *Environ. Pollut.* **2012,** *170*, 78-87.
(4) Masiol, M.; Harrison, R. M., Aircraft engine exhaust emissions and other airport-related contributions to ambient air pollution: A review. *Atmos. Environ.* **2014,** *95*, 409-455.
(5) Moore, R. H.; Shook, M.; Beyersdorf, A.; Corr, C.; Herndon, S.; Knighton, W. B.; Miake-Lye, R.; Thornhill, K. L.; Winstead, E. L.; Yu, Z. H.; Ziemba, L. D.; Anderson, B. E., Influence of Jet Fuel Composition on Aircraft Engine Emissions: A Synthesis of Aerosol Emissions Data from the NASA APEX, AAFEX, and ACCESS Missions. *Energy Fuels* **2015,** *29*, (4), 2591-2600.
(6) Brem, B. T.; Durdina, L.; Siegeris, F.; Beyerle, P.; Bruderer, K.; Rindlisbacher, T.; Rocci-Denis, S.; Andac, M. G.; Zelina, J.; Penanhoat, O.; Wang, J., Effects of Fuel Aromatic Content on Nonvolatile Particulate Emissions of an In-Production Aircraft Gas Turbine. *Environ. Sci. Technol.* **2015,** *49*, (22), 13149-13157.
(7) Cain, J.; DeWitt, M. J.; Blunck, D.; Corporan, E.; Striebich, R.; Anneken, D.; Klingshirn, C.; Roquemore, W. M.; Vander Wal, R., Characterization of Gaseous and Particulate Emissions From a Turboshaft Engine Burning Conventional, Alternative, and Surrogate Fuels. *Energy Fuels* **2013,** *27*, (4), 2290-2302.
(8) Corporan, E.; Edwards, T.; Shafer, L.; DeWitt, M. J.; Klingshirn, C.; Zabarnick, S.; West, Z.; Striebich, R.; Graham, J.; Klein, J., Chemical, Thermal Stability, Seal Swell, and Emissions Studies of Alternative Jet Fuels. *Energy Fuels* **2011,** *25*, (3), 955-966.
(9) Timko, M. T.; Yu, Z.; Onasch, T. B.; Wong, H. W.; Miake-Lye, R. C.; Beyersdorf, A. J.; Anderson, B. E.; Thornhill, K. L.; Winstead, E. L.; Corporan, E.; DeWitt, M. J.; Klingshirn, C. D.; Wey, C.; Tacina, K.; Liscinsky, D. S.; Howard, R.; Bhargava, A., Particulate Emissions of Gas Turbine Engine Combustion of a Fischer-Tropsch Synthetic Fuel. *Energy Fuels* **2010,** *24*, 5883-5896.
(10) ASTM D1655-17, *Standard Specification for Aviation Turbine Fuels*, **2017**.
(11) ASTM D7566-17a, *Standard Specification for Aviation Turbine Fuel Containing Synthesized Hydrocarbons*, **2017**.
(12) Gilham, R. J. J.; Quincey, P. G., Measurement and mitigation of response discontinuities of a widely used condensation particle counter. *J Aerosol Sci* **2009,** *40*, (7), 633-637.
(13) SAE AIR 6037, *Aircraft Exhaust Nonvolatile Particle Matter Measurement Method Development*, Beuth Verlag: Berlin, **2010**.
(14) EASA, ICAO Aircraft Engine Emissions Databank (www.easa.europa.eu, 01.06.2017). **2017**.
(15) Herndon, S.; Wood, E.; Franklin, J.; Miake-Lye, R.; Knighton, W. B.; Babb, M.; Nakahara, A.; Reynolds, T.; Balakrishnan, H., *Measurement of Gaseous HAP Emissions from Idling Aircraft as a Function of Engine and Ambient Conditions*. The National Academies Press: Washington, DC, 2012; p 101.
(16) Schripp, T.; Fauck, C.; Salthammer, T., Interferences in the determination of formaldehyde via PTR-MS: What do we learn from m/z 31? *Int J Mass Spectrom* **2010,** *289*, (2-3), 170-172.
(17) Arnold, F.; Kiendler, A.; Wiedemer, V.; Aberle, S.; Stilp, T.; Busen, R., Chemiion concentration measurements in jet engine exhaust at the ground: Implications for ion chemistry and aerosol formation in the wake of a jet aircraft. *Geophys. Res. Lett.* **2000,** *27*, (12), 1723-1726.
(18) Durdina, L.; Brem, B. T.; Abegglen, M.; Lobo, P.; Rindlisbacher, T.; Thomson, K. A.; Smallwood, G. J.; Hagen, D. E.; Sierau, B.; Wang, J., Determination of PM mass emissions from an aircraft turbine engine using particle effective density. *Atmos. Environ.* **2014,** *99*, 500-507.
(19) Mazaheri, M.; Johnson, G. R.; Morawska, L., Particle and Gaseous Emissions from Commercial Aircraft at Each Stage of the Landing and Takeoff Cycle. *Environ. Sci. Technol.* **2009,** *43*, (2), 441-446.

(20) Lobo, P.; Hagen, D. E.; Whitefield, P. D., Measurement and analysis of aircraft engine PM emissions downwind of an active runway at the Oakland International Airport. *Atmos. Environ.* **2012,** *61*, 114-123.
(21) Chan, T. W.; Chishty, W. A.; Canteenwalla, P.; Buote, D.; Davison, C. R., Characterization of Emissions From the Use of Alternative Aviation Fuels. *J. Eng. Gas. Turbines Power-Trans. ASME* **2016,** *138*, (1), 9.
(22) Petzold, A.; Fiebig, M.; Fritzsche, L.; Stein, C.; Schumann, U.; Wilson, C. W.; Hurley, C. D.; Arnold, F.; Katragkou, E.; Baltensperger, U.; Gysel, M.; Nyeki, S.; Hitzenberger, R.; Giebl, H.; Hughes, K. J.; Kurtenbach, R.; Wiesen, P.; Madden, P.; Puxbaum, H.; Vrchoticky, S.; Wahl, C., Particle emissions from aircraft engines - a survey of the European project PartEmis. *Meteorol. Z.* **2005,** *14*, (4), 465-476.
(23) Timko, M. T.; Onasch, T. B.; Northway, M. J.; Jayne, J. T.; Canagaratna, M. R.; Herndon, S. C.; Wood, E. C.; Miake-Lye, R. C.; Knighton, W. B., Gas Turbine Engine Emissions-Part II: Chemical Properties of Particulate Matter. *J. Eng. Gas. Turbines Power-Trans. ASME* **2010,** *132*, (6), 15.
(24) Vander Wal, R. L.; Bryg, V. M.; Huang, C. H., Aircraft engine particulate matter: Macro- micro- and nanostructure by HRTEM and chemistry by XPS. *Combust. Flame* **2014,** *161*, (2), 602-611.
(25) Stettler, M. E. J.; Boies, A. M.; Petzold, A.; Barrett, S. R. H., Global Civil Aviation Black Carbon Emissions. *Environ. Sci. Technol.* **2013,** *47*, (18), 10397-10404.
(26) ICAO *Airport Air Quality Manual (Doc. 9889)*; Quebec, Canada, 2011.
(27) Moore, R. H.; Thornhill, K. L.; Weinzierl, B.; Sauer, D.; D'Ascoli, E.; Kim, J.; Lichtenstern, M.; Scheibe, M.; Beaton, B.; Beyersdorf, A. J.; Barrick, J.; Bulzan, D.; Corr, C. A.; Crosbie, E.; Jurkat, T.; Martin, R.; Riddick, D.; Shook, M.; Slover, G.; Voigt, C.; White, R.; Winstead, E.; Yasky, R.; Ziemba, L. D.; Brown, A.; Schlager, H.; Anderson, B. E., Biofuel blending reduces particle emissions from aircraft engines at cruise conditions. *Nature* **2017,** *543*, (7645), 411-415.
(28) Christie, S.; Lobo, P.; Lee, D.; Raper, D., Gas Turbine Engine Nonvolatile Particulate Matter Mass Emissions: Correlation with Smoke Number for Conventional and Alternative Fuel Blends. *Environ. Sci. Technol.* **2017,** *51*, (2), 988-996.
(29) Law, M. E.; Westmoreland, P. R.; Cool, T. A.; Wang, J.; Hansen, N.; Taatjes, C. A.; Kasper, T., Benzene precursors and formation routes in a stoichiometric cyclohexane flame. *Proc. Combust. Inst.* **2007,** *31*, 565-573.
(30) Oßwald, P.; Whitside, R.; Schäffer, J.; Köhler, M., An experimental flow reactor study of the combustion kinetics of terpenoid jet fuel compounds: Farnesane, p-menthane and p-cymene. *Fuel* **2017,** *187*, 43-50.
(31) Zeng, M. R.; Li, Y. Y.; Yuan, W. H.; Li, T. Y.; Wang, Y. Z.; Zhou, Z. Y.; Zhang, L. D.; Qi, F., Experimental and kinetic modeling study of laminar premixed decalin flames. *Proc. Combust. Inst.* **2017,** *36*, (1), 1193-1202.
(32) McEnally, C. S.; Pfefferle, L. D.; Atakan, B.; Kohse-Höinghaus, K., Studies of aromatic hydrocarbon formation mechanisms in flames: Progress towards closing the fuel gap. *Prog. Energy Combust. Sci.* **2006,** *32*, (3), 247-294.
(33) Grohmann, J.; Rauch, B.; Kathrotia, T.; Meier, W.; Aigner, M., Influence of Single-Component Fuels on Gas-Turbine Model Combustor Lean Blowout. *J. Propul. Power* **2017**, 1-11.
(34) Oßwald, P.; Köhler, M., An atmospheric pressure high-temperature laminar flow reactor for investigation of combustion and related gas phase reaction systems. *Rev. Sci. Instrum.* **2015,** *86*, (10), 105-109.
(35) Bowden, T. T.; Pearson, J. H.; Wetton, R. J., The influence of fuel hydrogen content upon soot formation in a model gas-turbine combustor. *J. Eng. Gas. Turbines Power-Trans. ASME* **1984,** *106*, (4), 789-794.